33RD CONGRESS
OF THE INTERNATIONAL COUNCIL
OF THE AERONAUTICAL SCIENCES
STOCKHOLM, SWEDEN, 4-9 SEPTEMBER, 2022

EFFICIENT SURROGATE-BASED MULTI-OBJECTIVE OPTIMIZATION ALGORITHM WITH A NEW ADAPTIVE WEIGHT VECTOR GENERATION

Zuo Lu[1], Zhong-Hua Han[1], Zheng Zhou[2], Wen-Ping Song[1] & Yang Zhang[1]

[1]National Key Laboratory of Science and Technology on Aerodynamic Design and Research, Northwestern Polytechnical University, Xi'an, 710072, China
[2]Science and Technology on Scramjet Laboratory, CARDC, Mianyang Sichuan, 621000, China

Abstract

Most engineering design optimization problems are complex and expensive multi-objective optimization problems with multiple constraints. This paper proposes an improved surrogate-based multi-objective optimization algorithm (SBMO) using an adaptive weight vector generation method to address them. The main idea of the improved SBMO is to update the weight vectors of sub-problems adaptively according to the shape of the current Pareto front (PF) at each iteration while using SBMO to obtain Pareto optimal solutions. First, the improved SBMO decomposes a multi-objective optimization problem into a set of single-objective optimization sub-problems and builds surrogate models for each objective. Second, solutions are obtained by solving the acquisition problems for the sub-problems under the infill-sampling criteria. Third, all the solutions obtained will be evaluated and used to update the surrogate models to share the search information. At each iteration, the improved SBMO will divide the topology of the current PF evenly and select random points between the segment points. Well-distributed weight vectors will be generated based on the random points. This weight vector generation method can significantly improve the distribution of Pareto optimal solutions. The studies on benchmark test instances and aerodynamic design optimization of an airfoil indicate that the improved SBMO can obtain Pareto optimal solutions with better distribution than SBMO in a small number of sample points, and offers great potential to solve an expensive multi-objective optimization problem.

Keywords: multi-objective optimization; surrogate model; weight vectors; aerodynamic design optimization

1. Introduction

Engineering design optimization in the real world, like aerodynamic design optimization, is often formulated as a complex and expensive optimization problem with multiple objectives and constraints. Applying the existing multi-objective evolutionary algorithm to solve this problem is often suffered from the difficulty associated with high-fidelity numerical simulation such as computational fluid dynamics (CFD) or computational solid dynamics (CSD). Therefore, developing an optimization algorithm that can obtain good optimal solutions within a limited computational cost has great practical value for real-world engineering design optimization.

In the area of expensive optimization, it has been proved that using the surrogate model to replace the expensive numerical simulation is an effective way [1]. Besides the studies on single-objective problems, there have been some studies on extending the surrogate model to solve the expensive multi-objective problems [2]. In 2006, Knowles [3] proposed ParEGO, which extends the efficient global optimization method (EGO) [4] to the multi-objective problem by using the Tchebycheff approach to convert a multi-objective problem to several single-objective problems. Kanazaki [5] and Obayashi [6] et al. also proposed an extension of EGO, called multi-EGO, which obtains the Pareto optimal solutions and updates the surrogate models by applying the multi-objective genetic algorithm (MOGA) to optimize the expected improvement (EI) functions of objectives. Keane [7] and Emmerich [8] proposed multi-EI and expected hypervolume improvement (EHVI) infill-sampling criteria for multi-objective problems. With the assistance of surrogate models, those works significantly improved the efficiency of optimization compared to traditional multi-objective evolutionary algorithms. Those algorithms, however, can only obtain one candidate sample point at each iteration. In 2010, Zhang [9] proposed MOEA/D-EGO by introducing Kriging model (Gaussian stochastic process model) into MOEA/D to deal with the expensive multi-objective optimization, which can obtain a number of candidate sample points at one iteration. Lin [10] and Silva [11] further proposed MOBO/D and s-MOEA/D, respectively. These works further improved the efficiency and convergence of multi-objective optimization algorithms.

In 2019, Han and Liu [12] proposed a surrogate-based multi-objective optimization algorithm (SBMO) by combing surrogate-based optimization with the strategy of decomposition. The basic idea of SBMO is to decompose a multi-objective optimization problem into several single-objective optimization sub-problems and optimize them simultaneously, in which global surrogate models of each objective are used to enable full cooperation between sub-problems. The experimental studies on numerical cases show that SBMO is efficient, robust and has a good capability of constraint handling. And SBMO is successfully applied to multi-objective aerodynamic shape optimization of a transonic airfoil, offering its great potential to solve expensive multi-objective problems in real-world engineering design optimization.

This paper does further works on SBMO and the goal of this paper is to improve the distribution of Pareto optimal solutions obtained. Since SBMO is one of the algorithms under the Tchebycheff approach and uses weight vectors to guide the search direction of sub-problem optimization, the weight vector generation method plays a significant role in it. Reasonable distribution of weight vectors will lead to good distribution of Pareto optimal solutions. An improved SBMO is proposed in this paper, which uses an adaptive weight vector generation method we developed to obtain well-distributed Pareto optimal solutions.

The remainder of this paper is organized as follows. Section 2 presents the framework of the improved SBMO. Section 3 presents the experimental studies on numerical cases. Section 4 presents an aerodynamic design optimization of a wide-Mach-number-range airfoil using the improved SBMO. And section 5 is for the conclusions.

2. The Algorithm Framework

In this section, we will describe the framework of the improved SBMO. The definition of a multi-objective problem and the Tchebycheff decomposition approach will be described at first. Besides, we will discuss the developed adaptive weight vector generation method in detail.

2.1 The Tchebycheff Approach for Multi-Objective Problems

2.1.1 Multi-Objective Problems

A continuous multi-objective problem (MOP) can be defined generally as:

$$\begin{aligned} \min. \quad & \mathbf{F}(\mathbf{x}) = (f_1(\mathbf{x}), \cdots, f_m(\mathbf{x}))^{\mathrm{T}} \\ s.t. \quad & \mathbf{G}(\mathbf{x}) = \left(g_1(\mathbf{x}), \cdots, g_{n_g}(\mathbf{x})\right)^{\mathrm{T}} \geq 0 \\ & \mathbf{x} = (x_1, \cdots, x_k)^{\mathrm{T}} \in \Omega \end{aligned} \tag{1}$$

where $\mathbf{F}(\mathbf{x}) \to \mathbb{R}^m$ consists of m individual objective functions and $\mathbb{R}^m$ denotes the objective space. $\mathbf{G}(\mathbf{x})$ are n_g constraint functions. $\mathbf{x} = (x_1, \cdots, x_k)^{\mathrm{T}}$ is a decision variable which represents a solution to the target MOP and Ω is the k-dimensional decision space (or search space).

Let $\mathbf{x}_a, \mathbf{x}_b \in \Omega$ be two solutions of a MOP. $\mathbf{x}_a$ is said to dominate $\mathbf{x}_b$ if and only if $f_i(\mathbf{x}_a) \leq f_i(\mathbf{x}_b), \forall i \in \{1, \ldots, m\}$ and $f_j(\mathbf{x}_a) < f_j(\mathbf{x}_b), \exists j \in \{1, \ldots, m\}$. A solution $\mathbf{x}^* \in \Omega$ is called Pareto optimal if there is no other solution $\mathbf{x} \in \Omega$ dominating $\mathbf{x}^*$. The set of all the Pareto optimal solutions is called Pareto optimal set, denoted by PS. And the Pareto optimal front, denoted by PF, is defined as the collection of all the corresponding objective vectors of the solutions in PS.

2.1.2 The Tchebycheff Approach

There are several approaches had been developed to decompose a MOP into several single-objective sub-problems such as the weight sum approach, the Tchebycheff approach, the penalty-based

boundary intersection approach [13] and so on. Among these decomposition approaches, the Tchebycheff approach is the most widely used approach for its ability to solve MOPs with the non-convex Pareto optimal front.
A single-objective optimization sub-problem decomposed by the Tchebycheff approach can be formulated as:

$$\min_{\mathbf{x}\in\Omega} g^{tc}(\mathbf{x} \mid \lambda, \mathbf{z}^*) = \min_{\mathbf{x}\in\Omega} \max_{1\le i\le m} \{\lambda_i |f_i(\mathbf{x}) - z_i^*|\} \tag{2}$$

where $\lambda = (\lambda_1, \cdots, \lambda_m)$ is the weight vector of the sub-problem. $\mathbf{z}^* = (z_1, \cdots, z_m)$ is the reference point in objective space. In this paper, $z_i^* = \min\{\hat{f}_i(\mathbf{x})\}$, $\hat{f}_i(\mathbf{x})$ is the predictive value given by surrogate models of objectives.
A mapping vector λ' corresponding to the weight vector λ can be defined as:

$$\lambda' = WS(\lambda) = \left(\frac{\frac{1}{\lambda_1}}{\sum_{i=1}^m \frac{1}{\lambda_i}}, \frac{\frac{1}{\lambda_2}}{\sum_{i=1}^m \frac{1}{\lambda_i}}, \ldots, \frac{\frac{1}{\lambda_m}}{\sum_{i=1}^m \frac{1}{\lambda_i}} \right) \tag{3}$$

Notice that it is a self-inverse equation. That is, $\lambda = WS(\lambda') = WS(WS(\lambda))$. It has been proved that the optimal solution to the single-objective sub-problem with weight vector λ is the intersection of the PF and the mapping vector λ', if the intersection exists [14].

2.2 The Adaptive Weight Vector Generation Method

The objective of this paper is to improve the distribution of the Pareto optimal solutions on the PF. Since the optimal solution to a single-objective optimization sub-problem is the intersection of the mapping vector and the true PF, the distribution of mapping vectors has a serious impact on the distribution of the Pareto optimal solutions on the PF. Therefore, in order to obtain the optimal solutions with a good distribution on PF, well-distributed mapping vectors should be generated.
Recently, Dong and Wang [15] proposed a self-adaptive weight vector adjustment strategy based on chain segmentation. It regards the PF as a chain and generates the chain $\mathbf{C} = (c_1, \cdots, c_n)$ according to the topology of PF. Then it divides the chain evenly based on the Euclidean distance. And uniformly distributed weight vectors are generated from the reference point to the segment points. Although the chain segmentation strategy is a self-adaptive adjustment strategy for weight vectors, it also can be used to adjust mapping vectors. And in this paper, we used the current Pareto optimal solutions as an approximation to the true PF and update the mapping vectors based on the shape of the current approximated PF, since we do not know the shape of the true PF.
Moreover, since SBMO selects the Pareto optimal solutions from all evaluated sample points rather than the current population, the new sample points will be added in the same regions around the mapping vectors, which will result in the Pareto optimal solutions being crowded in the specific regions on the PF. Although the mapping vector adjustment strategy is introduced, this unexpected situation will still happen because the updated mapping vectors will be close to the old mapping vectors when the approximated PF is close to the true one. Therefore, it is necessary to introduce randomness into the adaptive weight vector generation method. In this paper, we select points randomly between the segment points after the chain segmentation strategy is used and generate the mapping vectors from the reference point to the random points. In this way, we can generate the uniformly distributed mapping vectors as far as possible, while the randomness is introduced.
Based on the above ideas, an adaptive weight vector generation method is proposed in this paper which works as Algorithm 1. And in the algorithm 1, $d(c_i, c_{i+1})$ represents the Euclidean distance between the adjacent points on the chain (c_i and c_{i+1}) and r is random value in $(0,1)$.

2.3 The Framework of the improved SBMO

The improved SBMO has the same framework as SBMO. The major differences between SBMO and the improved SBMO focus on the weight vector generation method. In addition to the initialization of weight vectors, the improved SBMO will update the weight vectors using the Algorithm 1 at each iteration during the search procedure.
The algorithm is summarized in Algorithm 2. The initialization method of weight vectors is the same as it in SBMO since there is no current approximated PF that can be used to apply the adaptive weight

Algorithm 1 The Adaptive Weight Vector Generation Method

Require: $PF_{current}$: the current approximated PF; N_w: the number of weight vectors (i.e. the number of sub-problems).

Ensure: $\lambda = (\lambda_1, \cdots, \lambda_{N_w})$: the weight vectors of sub-problems.

Step 1: Divide the current approximated PF as a chain.

Generate the chain $\mathbf{C} = (c_1, \cdots, c_n)$ based on the topology of $PF_{current}$ and calculate the length of C, $L = \sum_{i=1}^{n-1} d(c_i, c_{i+1})$. Then, divides the chain evenly in $l = L/N_w$. The segment points $(s_1, \cdots, s_{N_w+1})$ are generated.

Step 2: Generate the mapping vectors.

Select random points $\mathbf{q}$ between the adjacent segment points and generate mapping vectors from the reference point $\mathbf{z}^*$ to $\mathbf{q}$:

for $i = 1; i < N_w$ **do**

$\mathbf{q}^i = s_i + r(s_{i+1} - s_i)$, $r = random(0,1)$

$\lambda'_i = \mathbf{q}^i - \mathbf{z}^*$

end for

Step 3: Generate the weight vectors.

Transform the mapping vectors $\lambda' = (\lambda'_1, \cdots, \lambda'_{N_w})$ into the weight vectors $\lambda = (\lambda_1, \cdots, \lambda_{N_w})$ by the Equation 3. It would be calculated as:

$$\lambda_i = WS(\lambda'_i) = \left(\frac{\frac{1}{q_1^i - z_1^*}}{\sum_{j=1}^{m} \frac{1}{q_j^i - z_j^*}}, \frac{\frac{1}{q_2^i - z_2^*}}{\sum_{j=1}^{m} \frac{1}{q_j^i - z_j^*}}, \ldots, \frac{\frac{1}{q_m^i - z_m^*}}{\sum_{j=1}^{m} \frac{1}{q_j^i - z_j^*}} \right)$$

vector generation method. It is noticed that the weight vectors $(0,1),(1,0)$ (for bi-objective problem) should be added to avoid the reduction of search space. As a result, there are $N_w - 2$ weight vectors exactly generated by the adaptive weight vector generation method.

In the improved SBMO, we use the Kriging model [16] as the surrogate model. And the acquisition problems for sub-problems are defined by the infill-sampling criteria. In this paper, the minimizing surrogate prediction (MSP) and the expected improvement (EI) [17]infill-sampling criteria are both used. In the case of a bi-objective problem ($m = 2$), the acquisition problem for i-th sub-problem ($\xi^i(\mathbf{x})$) is defined as follows.

- Infill-sampling criterion of MSP.

$$\begin{aligned} \min. \quad & \xi^i(\mathbf{x}) = \max\left\{\lambda_1^i\left(\hat{f}_1(\mathbf{x}) - z_1^*\right), \lambda_2^i\left(\hat{f}_2(\mathbf{x}) - z_2^*\right)\right\} \\ s.t. \quad & \hat{G}(\mathbf{x}) = \left(\hat{g}_1(\mathbf{x}), \cdots, \hat{g}_{n_g}(\mathbf{x})\right)^T \geq 0 \\ & \mathbf{x} = (x_1, \cdots, x_k)^{\mathrm{T}} \in \Omega \end{aligned} \tag{4}$$

where $\hat{f}(\mathbf{x})$ and $\hat{g}(\mathbf{x})$ denote the value predicted by Kriging models for the objectives and constraints, respectively.

- Infill-sampling criterion of EI.

$$\begin{aligned} \min. \quad & \xi^i(\mathbf{x}) = E^i[I(\mathbf{x})] \cdot \prod_{j=1}^{n_g} P\left[G_j \geq 0\right] \\ s.t. \quad & \mathbf{x} = (x_1, \cdots, x_k)^{\mathrm{T}} \in \Omega \end{aligned} \tag{5}$$

where the EI function $E^i[I(\mathbf{x})]$ is defined as:

$$E^i[I(\mathbf{x})] = \begin{cases} \left[g_{\min}^{tc,i} - \hat{g}^{tc,i}(\mathbf{x})\right]\Phi\left(\frac{g_{\min}^{tc,i} - \hat{g}^{tc,i}(\mathbf{x})}{\hat{s}^i(\mathbf{x})}\right) + \hat{s}^i(\mathbf{x})\phi\left(\frac{g_{\min}^{tc,i} - \hat{g}^{tc,i}(\mathbf{x})}{\hat{s}^i(\mathbf{x})}\right) & , \hat{s}^i(\mathbf{x}) > 0 \\ 0 & , \hat{s}^i(\mathbf{x}) = 0 \end{cases} \tag{6}$$

where Φ and ϕ represent the cumulative distribution and probability density function of a standard normal distribution, respectively. $\hat{g}^{tc,i}$ is the value of i-th sub-problem calculated with the prediction given by Kriging models for the objectives and constraints and $g_{\min}^{tc,i}$ is the minimum value among the evaluated sample points.

And $P[G_j \geq 0]$ is the probability of satisfying the constraint at any site, which is defined as:

$$P[G_j(\mathbf{x}) \geq 0] = 1 - \Phi\left(-\frac{\hat{g}_j(\mathbf{x})}{s_{g,j}(\mathbf{x})}\right), j = 1, \cdots, n_g \quad (7)$$

where $s_{g,j}(\mathbf{x})$ is the standard derivation of $G_j(\mathbf{x})$, which is assumed as normally distributed.

Algorithm 2 The improved SBMO

Require: N_I: the number of initial sample points; N_w: the number of sub-problems (i.e. the number of weight vectors); N_{max}: the maximum number of evaluated sample points.

Ensure: The final set of the Pareto optimal solutions P_{eval}.

Step 1: Initial sampling and evaluations.

Generate N_I initial sample points by using a design of experiments method (DoE) and evaluate them by running expensive numerical simulations.

Step 2: Initial surrogate models and weight vectors.

Establish the Kriging models for each objective $(\hat{f}_1, \cdots, \hat{f}_m)$ based on the initial sample points and their response. And weight vectors also would be initialized in this step.

Step 3: Update.

Step 3.1: Solve acquisition problems to suggest new sample points.

The acquisition problems are defined as $\xi^i(\mathbf{x})$ for i-th sub-problem. Some well-developed single-objective optimization algorithms are used to solve the acquisition problems and N_w new sample points will be suggested in turn.

Step 3.2: New sample point evaluations.

N_w new sample points are evaluated by expensive simulations using parallel computing and the resulting data is augmented to P_{eval}.

Step 3.3: Update the Kriging model and the weight vectors.

if N_P (The number of P_{eval}) $\geq N_{max}$ **then**

  Go to **Step 4**.

else

  Update the Kriging model by the P_{eval}.

  Update the weight vectors by the adaptive weight vector generation method (Algorithm 1).

  Go to **Step 3.1**.

end if

Step 4: Output.

Record all the information at each iteration and output P_{eval}.

---

3. Validation and Comparison

In this section, we will employ the improved SBMO to solve several numerical multi-objective problems and compare the results with SBMO.

3.1 Test instance

In this experimental study, we select four widely used bi-objective ZDT test instances and two bi-objective test instances with constraints, SRN and TNK [18]. The information of these test instances is shown in table 1.

3.2 Performance Metric

In this paper, we use the inverted generational distance (IGD) metric and hypervolume difference HV_I metric [19] which are comprehensive metrics of convergence and diversity that can measure the performance of a multi-objective algorithm.

Table 1 – List of the selected test instances.

Instances	No. of variables	No. of objectives	No. of constraints	Feature of PF
ZDT1	8	2	0	convex and continuous
ZDT2	8	2	0	nonconvex and continuous
ZDT3	8	2	0	convex and discontinuous
ZDT6	8	2	0	nonconvex and continuous
SRN	2	2	2	continuous
TNK	2	2	2	discontinuous

- The IGD metric is defined as:

$$\mathrm{IGD}\left(P^{*},P\right)=\frac{\sum_{v\in P^{*}}d\left(v,P\right)}{\left|P^{*}\right|} \tag{8}$$

  where P^{*} is a set of evenly distributed points over the PF in the objective space, and v is a point in P^{*}. P denotes a set of Pareto optimal solutions which is obtained by an algorithm. $\mid P^{*}\mid$ represent the number of points in P^{*} and when $\mid P^{*}\mid$ is large enough, $\mathrm{IGD}\left(P^{*},P\right)$ can evaluate both the convergence and the diversity of P. The lower value of IGD indicates that P is closer to the PF and has a better distribution on the PF.

- The HV_I metric is defined as:

$$\begin{gathered} HV=\delta\left(\bigcup_{i=1}^{N}v_i\right) \\ HV_I=HV_{PF}-HV_{nond} \end{gathered} \tag{9}$$

  where δ is the Lebesgue measure and v_i is the hypervolume of i-th point in the set of Pareto optimal solutions. HV_{PF} and HV_{nond} represent the hypervolume of the PF and the Pareto optimal solutions obtained by an algorithm, respectively. The lower value of HV_I also indicates that the Pareto optimal solutions obtained is closer to the PF and has a better distribution on the PF.

3.3 Parameter Settings

In this experimental study, the parameter settings of the improved SBMO and SBMO are set as follows.

- The number of initial sample points N_I is set to $10k+1$ for all the instances, where k represents the number of design variables. And the design of experiments is Latin hypercube sampling (LHS).
- The maximum number of evaluation iterations N_{max} is set to 200 for all the instances.
- The number of weight vectors N_w is set to 12. There are two weight vectors $(1,0)$ and $(0,1)$, which apply the EI infill-sampling criteria. And the other 10 weight vectors apply the MSP infill-sampling criteria, which are generated by LHS in SBMO and by the adaptive weight vector generation method (Algorithm 1) in the improved SBMO.

3.4 Experimental Results

In this paper, we run 10 times independently with different random initial points for each test instance. Table 2 and 3 present the mean of the IGD metric value and the HV_I metric value of the final Pareto optimal solutions obtained by SBMO and the improved SBMO for all the instances over 10 independent runs, respectively.
It is evident that the improved SBMO performs better than SBMO in the test instances with complex PF. In the ZDT3 and TNK which have a discontinuous PF, both IGD and HV_I metric value of the Pareto optimal solutions obtained by the improved SBMO is better than that obtained by SBMO. And the improved SBMO also performs better in the ZDT6, although it has lower value of IGD in the

ZDT2 and performs worse in the ZDT1. Figure 1 shows the Pareto optimal solutions in design space obtained by the improved SBMO for all the test instances.

Table 2 – Statistic IGD metric value of the Pareto optimal solutions obtained by the improved SBMO and SBMO.

Instances	ZDT1	ZDT2	ZDT3	ZDT6	SRN	TNK
SBMO	**0.0079**	**0.0082**	0.0232	0.0648	**1.2258**	0.0179
The improved SBMO	0.0087	0.0103	**0.0203**	**0.0545**	1.2322	**0.0162**

Table 3 – Statistic HV_I metric value of the Pareto optimal solutions obtained by the improved SBMO and SBMO .

Instances	ZDT1	ZDT2	ZDT3	ZDT6	SRN	TNK
SBMO	**0.0118**	0.0097	0.0069	0.0563	**0.0045**	0.0116
The improved SBMO	0.0125	**0.0091**	**0.0064**	**0.0492**	0.0050	**0.0113**

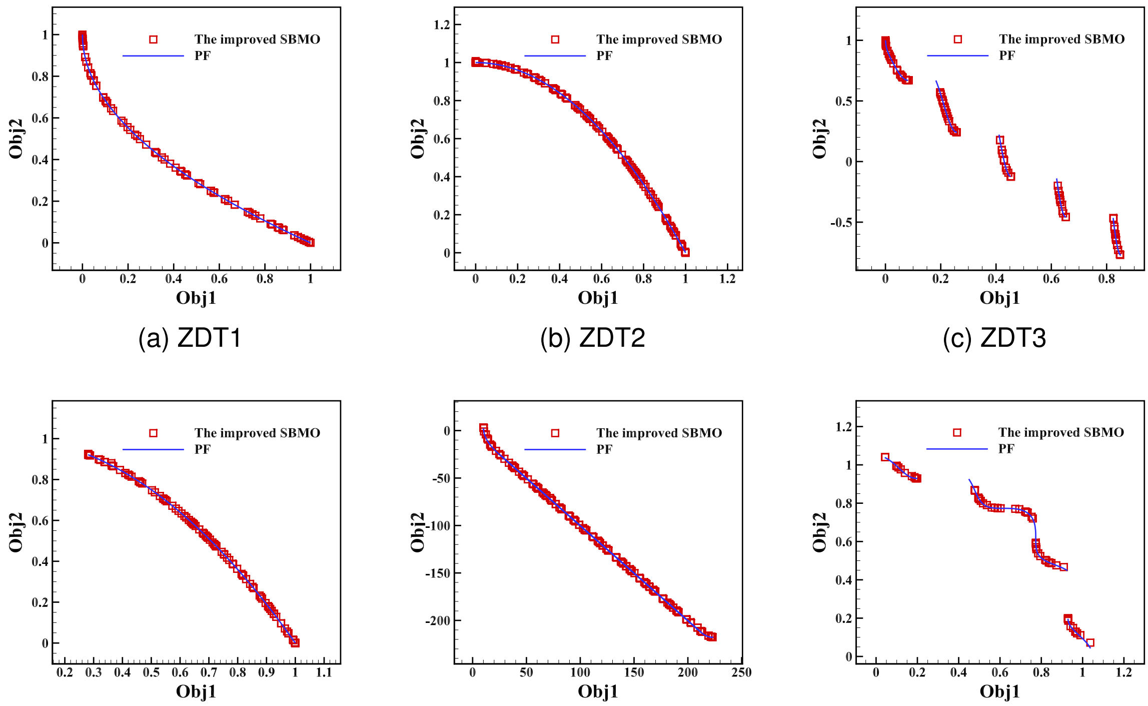

(a) ZDT1 (b) ZDT2 (c) ZDT3

(d) ZDT6 (e) SRN (f) TNK

Figure 1 – The Pareto optimal solutions obtained by the improved SBMO for all the test instances.

4. Aerodynamic Design Optimization of an Airfoil Using SBMO-AW

In this section, the improved SBMO will be applied to a wide-Mach-number-range airfoil design optimization. Wide-Mach-number-range airfoil design optimization is a typical multi-objective optimization since it has a conflict between the lift-to-drag ratios under transonic and hypersonic.

4.1 Problem Description

In this airfoil design optimization, we choose NACA64A-204 as the baseline airfoil and regard the lift-to-drag ratios under transonic and hypersonic as two objectives to optimize. The design points are $Ma = 0.8, Re = 7.6 \times 10^6, \alpha = 1.5^\circ$ and $Ma = 6.0, Re = 4.23 \times 10^6, \alpha = 5^\circ$, where Ma means Mach number, Re means chord Reynold number and α means the angle of attack.

The optimization problem is defined as

$$\begin{aligned} \max. \quad & f_1 = (L/D)_{Ma=0.8} \\ & f_2 = (L/D)_{Ma=6} \\ s.t. \quad & \mid t - t_{baseline} \mid \leq 0.02 \times t_{baseline} \end{aligned} \tag{10}$$

where, $(L/D)_{Ma=0.8}$ and $(L/D)_{Ma=0.8}$ represent the lift-to-drag ratios at $Ma = 0.8$ and $Ma = 6.0$ respectively. t represents the maximum thickness respect to chord of airfoil. And the variable with subscript "baseline" represents that of the baseline airfoil.
Since we apply the eighth-order class-function shape-function transformation (CST) [20] method to perturb the shape of an airfoil, the number of design variables comes to 18. 100 initial sample points are generated by LHS and evaluated by our in-house RANS flow solver. At each generation, 12 new sample points are generated and added to update the Kriging models, in which 2 sample points are generated by EI infill-sampling criteria and 10 sample points are generated by MSP infill-sampling criteria. The optimization will stop when the total number of evaluated points reaches 400.

4.2 Optimization Result

Figure 2 shows the approximated PF found by the improved SBMO. There are 68 Pareto optimal solutions found in 400 evaluated points with all the constraints being strictly satisfied. The comparison of objectives and constraints of three selected optimal airfoils and the baseline airfoil is shown in Table 4. It can be seen that the Opt 1 and Opt 3 airfoils have the best lift-drag-ratio value at one objective while having a little improvement or even getting worse at another objective. And the Opt 2 balances the lift-drag-ratios under transonic and hypersonic. Designers can select the optimal airfoil as their wish and analyze the relationship between objectives, which will significantly contribute to the improvement of the aerodynamic design. Figure 3 gives a comparison of pressure coefficient distributions of three selected optimal airfoils on the approximated PF with that of the baseline airfoil.

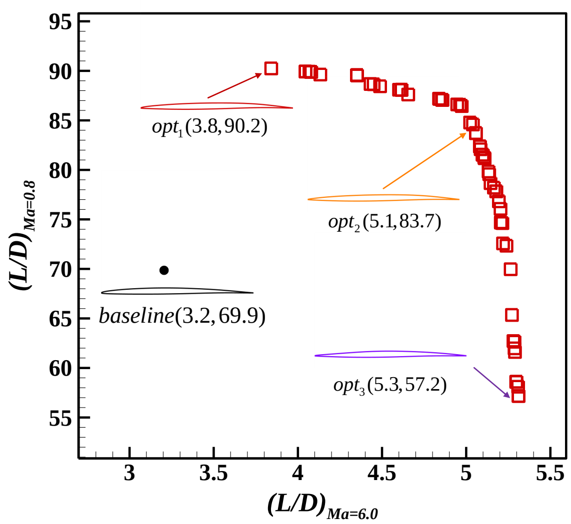

Figure 2 – Final Pareto optimal solutions obtained by the improved SBMO in the objective space for multi-objective optimization of an airfoil.

5. Conclusion

In this paper, we proposed an improved SBMO using an adaptive weight vector generation method to obtain Pareto optimal solutions with better distribution. The basic idea of the adaptive weight vector generation method is to generate well-distributed weight vectors based on the shape of the current approximated PF. In this paper, we generated mapping vectors by uniformly distributed segments

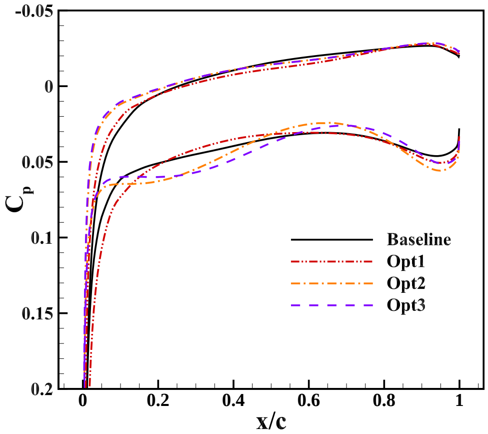

(a) $Ma = 6.0, Re = 4.23 \times 10^6, \alpha = 5^\circ$

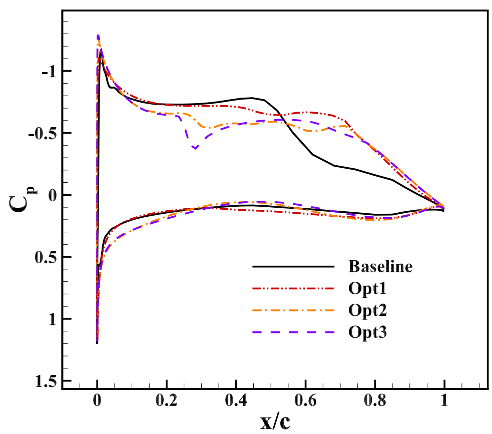

(b) $Ma = 0.8, Re = 7.6 \times 10^6, \alpha = 1.5^\circ$

Figure 3 – Comparison of pressure coefficient distributions of three selected optimal airfoils and the baseline airfoils.

Table 4 – Comparison of objectives and constraints of selected optimal airfoils and the baseline airfoils.

Airfoil	Objectives		Constrations	
	$(L/D)_{Ma=6.0}$	$(L/D)_{Ma=0.8}$	t	$\lvert t - t_{baseline} \rvert / t_{baseline}$
Baseline	3.2	69.9	0.0400	
Opt1	3.8(+18.75%)	90.2(+29.04%)	0.0394	0.015<0.02
Opt2	5.1(+59.38%)	83.7(+19.74%)	0.0396	0.010<0.02
Opt3	5.3(+65.63%)	57.2(-18.17%)	0.03922	0.0195<0.02

on the topology of the current approximated PF and transform the mapping vectors into the weight vectors. Randomness is also introduced into the weight vector generation method to avoid new sample points being added in the same regions as the last iteration. We compared the improved SBMO with SBMO in four well-known ZDT instances and two instances with constraints (SRN and TNK). And the improved SBMO was also employed for aerodynamic design optimization of a wide-Mach-number-range airfoil.

The results of experimental studies on numerical cases indicated that the improved SBMO is able to obtain a well-converged and well-distributed set of Pareto optimal solutions. And the metrics of Pareto optimal solutions indicated that the improved SBMO performs better than SBMO on the test instances with complex PF. The study on aerodynamic design optimization indicated that the improved SBMO can find a set of Pareto optimal solutions in a limited number of evaluated sample points, which will significantly contribute to the improvement of the aerodynamic design. The aerodynamic design optimization showed that the improved SBMO has great potential to solve expensive multi-objective problems in real-world engineering design optimization.

There are still more works that need to be done in the future, such as a study on other infill-sampling criteria and the way how to combine different criteria. Further improvements to the weight vector generation method also should be studied, such as how to figure the discontinuous part on the PF out for the MOP with a discontinuous PF. The other processing in SBMO such as selecting the candidate points in each generation and building the global surrogate models are also worth being studied. And we will also focus on the works on the application of SBMO to real-world engineering problems, such as aerodynamic shape design optimization for aerospace engineering.

6. Acknowledgment

This research was sponsored by the National Natural Science Foundation of China grant Nos. U20B2007, the Shaanxi Science Fund for Distinguished Young Scholars under grant No. 2020JC-13, the Shaanxi Science Fund under grand No. 2020JM-127 and the "111" project of China No. B17037.

7. Contact Author Email Address

Zhong-Hua Han, Professor, hanzh@nwpu.edu.cn, corresponding author.

8. Copyright Statement

References

[1] Han Z H. SurroOpt: a generic surrogate-based optimization code for aerodynamic and multidisciplinary design. *Proceedings of ICAS 2016*, 2016.

[2] Jin Y, Wang H, Chugh T, Guo D, and Miettinen K. Data-Driven Evolutionary Optimization: An Overview and Case Studies. *IEEE Transactions on Evolutionary Computation*, Vol 23, No. 3, pp 442–458, 2019.

[3] Knowles J. ParEGO: a hybrid algorithm with on-line landscape approximation for expensive multiobjective optimization problems. *IEEE Transactions on Evolutionary Computation*, Vol 10, No. 1, pp 50–66, 2006.

[4] Jones D R, Schonlau M, and Welch W J. Efficient Global Optimization of Expensive Black-Box Functions. *Journal of Global Optimization*, Vol 13, No. 4, pp 455–492, 1998.

[5] Kanazaki M, Jeong S, Tanaka K, and Yamamoto K. Multi-Objective Aerodynamic Exploration of Elements Setting for High-Lift Airfoil Using Kriging Model. *Journal of the Japan Society for Aeronautical and Space Sciences*, Vol 54, No. 632, pp 419–426, 2006.

[6] Obayashi S, Sasaki D, Takeguchi Y, and Hirose N. Multiobjective evolutionary computation for supersonic wing-shape optimization. *IEEE Transactions on Evolutionary Computation*, Vol 4, No. 2, pp 182–187, 2000.

[7] Keane A J. Statistical improvement criteria for use in multiobjective design optimisation. *AIAA Journal*, Vol 44, pp 879–891, 2006.

[8] Emmerich M, Giannakoglou K, and Naujoks B. Single- and multiobjective evolutionary optimization assisted by Gaussian random field metamodels. *IEEE Transactions on Evolutionary Computation*, Vol 10, No. 4, pp 421–439, 2006.

[9] Zhang Q, Liu W, Tsang E, and Virginas B. Expensive Multiobjective Optimization by MOEA/D With Gaussian Process Model. *IEEE Transactions on Evolutionary Computation*, Vol 14, No. 3, pp 456–474, 2010.

[10] Lin X, Zhang Q, and Kwong S. An efficient batch expensive multi-objective evolutionary algorithm based on Decomposition. *2017 IEEE Congress on Evolutionary Computation (CEC)*, pp 1343–1349, Donostia, San Sebastián, Spain, 2017. IEEE Press.

[11] Silva R C P, Li M, Rahman T, and Lowther D A. Surrogate-Based MOEA/D for Electric Motor Design With Scarce Function Evaluations. *IEEE Transactions on Magnetics*, Vol 53, pp 2661987, 2017.

[12] Han Z, Liu F, Xu C, Zhang K, and Zhang Q. Efficient Multi-Objective Evolutionary Algorithm for Constrained Global Optimization of Expensive Functions. *2019 IEEE Congress on Evolutionary Computation (CEC)*, pp 2026–2033, 2019.

[13] Zhang Q and Hui L. MOEA/D: A Multiobjective Evolutionary Algorithm Based on Decomposition. *IEEE Transactions on Evolutionary Computation*, Vol 11, No. 6, pp 712–731, 2008.

[14] Qi Y, Ma X, Liu F, Jiao L, Sun J, and Wu J. MOEA/D with Adaptive Weight Adjustment. *Evolutionary Computation*, Vol 22, No. 2, pp 231–264, 2014.

[15] Dong Z, Wang X, and Tang L. MOEA/D with a self-adaptive weight vector adjustment strategy based on chain segmentation. *Information Sciences*, Vol 521, pp 209–230, 2020.

[16] Han Z H, Görtz S, and Zimmermann R. Improving variable-fidelity surrogate modeling via gradient-enhanced kriging and a generalized hybrid bridge function. *Aerospace Science and Technology*, Vol 25, No. 1, pp 177–189, 2013.

[17] Han Z, Xu C, Zhang L, Zhang Y, Zhang K, and Song W. Efficient aerodynamic shape optimization using variable-fidelity surrogate models and multilevel computational grids. *Chinese Journal of Aeronautics*, Vol 33, No. 1, pp 31–47, 2020.

[18] Deb K, Pratap A, Agarwal S, and Meyarivan T. A fast and elitist multiobjective genetic algorithm: NSGA-II. *IEEE Transactions on Evolutionary Computation*, Vol 6, No. 2, pp 182–197, 2002.

[19] Zitzler E, Thiele L, Laumanns M, Fonseca C, and da Fonseca V. Performance assessment of multiobjective optimizers: an analysis and review. *IEEE Transactions on Evolutionary Computation*, Vol 7, No. 2, pp 117–132, 2003.

[20] Kulfan B M. Universal Parametric Geometry Representation Method. *Journal of Aircraft*, Vol 45, No. 1, pp 142–158, 2008.